JOURNAL OF APPLIED SPECTROSCOPY SEPTEMBER — OCTOBER 2021

АННОТАЦИИ АНГЛОЯЗЫЧНЫХ СТАТЕЙ **

ENHANCED UP-CONVERSION OF HIGH CONCENTRATION Yb³+/Er³+ DOPED $\beta\text{-Na}\text{YF}_4$ MICROPARTICLES BY CHANGING THE HOST MATRIX

Q. Bo, J. Wang*

School of Physics at Beihang University, 100191 Beijing, China; e-mail: wangjinliang@buaa.edu.cn

With the aim of improving the up-conversion luminescence intensity of high concentration Yb^{3+}/Er^{3+} doped microparticles, Yb^{3+}/Er^{3+} doped β -NaYF₄/ β -NaLuF₄/ β -NaYbF₄ samples were prepared by the hydrothermal method. X-ray diffraction (XRD) and scanning electron microscopy (SEM) were used to characterize the crystal structure and morphology. Intense blue emission (${}^2H_{11/2} \rightarrow {}^4I_{15/2}$), ${}^4S_{3/2} \rightarrow {}^4I_{15/2}$) and red emission (${}^4F_{9/2} \rightarrow {}^4I_{15/2}$) of Er^{3+} were observed under 980 nm excitation. When the doping concentrations of Yb^{3+} and Er^{3+} were high, the up-conversion luminescence intensity using β -NaYbF₄ as the host matrix was enhanced, and in the experiment the sample NaYbF₄:16 mol%Yb³⁺/32 mol%Er³⁺ with β -NaYbF₄ as the host matrix has the strongest luminescence.

Keywords: rare-earth, up-conversion, β -NaYb F_4 .

УСИЛЕНИЕ АП-КОНВЕРСИИ МИКРОЧАСТИЦ β-NaYF₄, ДОПИРОВАННЫХ ИОНАМИ Yb³⁺/Er³⁺ ВЫСОКОЙ КОНЦЕНТРАЦИИ ЗА СЧЕТ ИЗМЕНЕНИЯ БАЗОВОЙ МАТРИЦЫ-ХОЗЯИНА

Q. Bo, J. Wang*

УДК 535.37

Школа физики Университета Бэйхан, 100191, Пекин, Китай; e-mail: wangjinliang@buaa.edu.cn

(Поступила 16 марта 2020)

Для повышения интенсивности ап-конверсионной люминесценции гидротермальным методом приготовлены образцы β -NaYF4/ β -NaLuF4/ β -NaYbF4, легированные ионами высокой концентрации Yb^{3+}/Er^{3+} . Для характеризации их кристаллической структуры и морфологии использованы дифракция рентгеновских лучей (XRD) и сканирующая электронная микроскопия (SEM). При возбуждении на $\lambda = 980$ нм наблюдаются интенсивные полосы синего ($^2H_{11/2} \rightarrow ^4I_{15/2}$, $^4S_{3/2} \rightarrow ^4I_{15/2}$) и красного излучения ($^4F_{9/2} \rightarrow ^4I_{15/2}$) ионов Er^{3+} . При высоких концентрациях легирования Yb^{3+} и Er^{3+} интенсивность апконверсионной люминесценции с использованием β -NaYbF4 в качестве матрицы увеличивается; образец NaYbF4:16 мол.% $Yb^{3+}/32$ мол.% Er^{3+} с β -NaYbF4 в качестве матрицы в эксперименте обладает сильнейшим свечением.

Ключевые слова: редкоземельный элемент, ап-конверсия, β -NaYbF₄.

Introduction. Lanthanide ions have been used in up-conversion (UC) of luminescent materials [1–3]. RE doped materials have many applications in optical communications [4], photocatalysis [5], biomedicine [6], color displays, etc. [7–11]. At the same time, one knows the concentration fluorescence quenching effect, which is a decrease in the emission of the phosphor with increase in the concentration of the doped rare earth

^{**}Full text is published in JAS V. 88, No. 5 (http://springer.com/journal/10812) and in electronic version of ZhPS V. 88, No. 5 (http://www.elibrary.ru/title_about.asp?id=7318; sales@elibrary.ru).

(RE) ion [12]. The reasons for that are the existence of quenching centers such as remote killers, the crystal surface, significant nonradiative energy loss during cross-relaxation, and the resonance between the activators [13]. The Yb³⁺ ion doped as the sensitizer is used to enhance the pump efficiency of the activators such as Er³⁺, Tm³⁺, and Ho³⁺ [14–18]. The materials co-doped with Li⁺ can improve the UC emission intensity [19–21]. Aluminum oxynitride (AlON) as the host material can improve the UC emission intensity with low phonon energy for weakening the possibility of nonradiative transitions, and it also demonstrated a new strategy to remarkably improve the up-conversion luminescence by an active-core/luminescent-shell/active-shell engineering technique [22–28].

In this paper, high concentration β -NaYF₄:16 mol%Yb³⁺, 32 mol%Er³⁺ microparticles were synthesized by a facile hydrothermal method. It was indicated that when the host matrix was changed from β -NaYF₄ to β -NaYbF₄, the up-conversion luminescence intensity of the 16 mol%Yb³⁺, 32 mol%Er³⁺ doped phosphor was enhanced significantly. This can be an effective method to inhibit the concentration quenching.

Experimental. As starting materials, NaF (98%) and $C_{10}H_{16}N_2O_8$ (EDTA) were purchased from Shanghai Macklin Biochemical Co., Ltd. (China); Y(NO₃)₃·6H₂O(99.99%), Yb(NO₃)₃·6H₂O(99.99%), Er(NO₃)₃·6H₂O(99.99%), and Lu(NO₃)₃·6H₂O (99.99%) were purchased from Shanghai Diyang Chemical Co., Ltd. (China). They were all used without further purification.

The samples NaYF₄:32 mol%Er³⁺, NaYF₄:8 mol%Yb³⁺/32 mol%Er³⁺, NaYF₄:16 mol%Yb³⁺/32 mol%Er³⁺, NaYF₄:32 mol%Er³⁺, NaYbF₄:16 mol%Yb³⁺/32 mol%Er³⁺, NaYbF₄:16 mol%Yb³⁺/32 mol%Er³⁺, and NaYbF₄:32 mol%Er³⁺ named Er 32%, a, b, c, d, e, f, respectively, were prepared by the hydrothermal method. Appropriate amounts of Y(NO₃)₃·6H₂O, Lu(NO₃)₃·6H₂O and Yb(NO₃)₃·6H₂O were dissolved in deionized water to form the host, and then 32 mol%Er(NO₃)₃·6H₂O and xmol% Yb(NO₃)₃(x = 8, 16, 32) relative to the moles of Y(NO₃)₃·6H₂O, Yb(NO₃)₃·6H₂O or Lu(NO₃)₃·6H₂O were dissolved in deionized water. They were immediately added into an aqueous solution of EDTA with vigorous magnetic stirring, and an aqueous solution of NaF was then added, stirred for 1 h, and the lanthanide used to synthesize the host/EDTA/NaF with a molar ratio of 1/1/12. The as-obtained mixing solution was poured into a 50 mL Teflon-lined autoclave and heated for 2 h at 180°C. The white precipitates were separated by centrifugation, washed three times with deionized water and ethanol in sequence, and then dried at 80°C.

Phase analysis of the samples was characterized using a Rigaku Model D/max-2200 (CuK_{α} λ = 0.15418 nm) in the range from 10° to 70° with a scanning step size of 0.02°. The size and morphology of the samples were characterized by a field emission scanning electron microscope (SEM) (GeminiSEM 500). The energy dispersive X-ray (EDX) spectrum of the samples was characterized by a field emission scanning electron microscope (SEM) (JEOL JSM-6700F). The up-conversion emission spectra and the luminescence decay curves were recorded by an FLS980 spectrometer (Edinburgh) with conducted 980 nm fiber lasers as excitation sources, the power of the 980 nm fiber laser being 0.95 W. All the measurements were performed at room temperature.

Results and discussion. The typical XRD patterns for some selected samples are shown in Fig. 1. All the diffraction peaks correspond to the (100), (110), (101), (200), (111), (201), (210), (002), (300), (211), (102), (112), (220), (202), and (310) planes, and they can be indexed to the pure NaYF₄ hexagonal phase reported in JCPDS card No. 16-0334. β-NaYF₄:Yb,Er co-doped with different amounts of Yb³⁺ ions, were recorded as Er 32%, a, b, c with the same phase structure. As the host lattice of samples d and e, β-NaLuF₄ and β-NaYbF₄ are isostructural with β-NaYF₄, and they present a hexagonal structure. In the patterns, no additional diffraction peaks were observed.

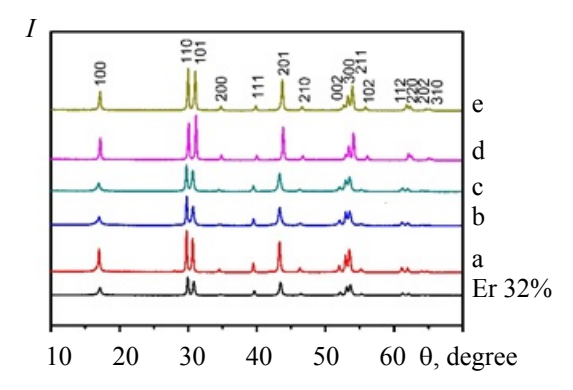
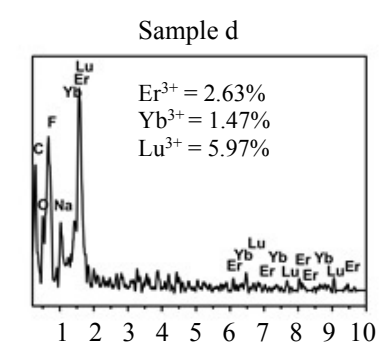


Fig. 1. XRD patterns of samples Er 32%, a, b, c, d, e.

The EDX spectra of samples d and e are presented in Fig. 2. The EDX spectra show strong peaks of C, O, F, Na, Er, Lu, and Yb containing 2.63 mol% Er³⁺, 1.47 mol% Yb³⁺, 5.97 mol%Lu³⁺ in sample d, and 2.35 mol% Er³⁺, 8.21 mol% Yb³⁺ in sample e, respectively. This indicates that Er³⁺, Yb³⁺, and Lu³⁺ ions concentrate mainly inside the crystal.



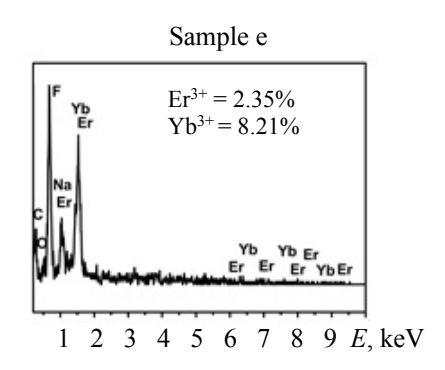


Fig. 2. EDX of samples d and e.

Figure 3 displays the SEM images of the samples. From Fig. 3a–c, it can be seen that β -NaYF₄:8 mol% Yb³⁺, 32 mol% Er³⁺ particles have uniform hexagonal prism morphology with a length of 2 μm and a bottom side length of 200–500 nm. When the Yb³⁺ doping concentration increases from 8 to 32 mol%, the morphology of the samples becomes irregular and small. The SEM image of β -NaLuF₄:16 mol% Yb³⁺, 32 mol% Er³⁺, as shown in Fig. 3d, demonstrates some nearly spherical particles with a length of 300 nm. The SEM image of β -NaYbF₄:16 mol% Yb³⁺, 32 mol% Er³⁺ is shown in Fig. 3e. It is observed that the sample is composed of hexagonal prisms with an edge length of 600 nm and a bottom side length of 300 nm. In the synthesis process of the samples, by binding Ln³⁺ and releasing Ln³⁺ continuously, EDTA controlled the process [29]. The growth rate of the particles controlled by solute reactions on the surface is proportional to their surface area, which results in an uneven particle size.



Fig. 3. SEM images of samples a, b, c, d, e.

UC luminescent spectra analysis. As shown in Fig. 4A, the synthesized samples exhibited green and red emission under 980 nm excitation. The sample Er 32%, a, b, c has similar emission with peaks at 521 and 540 nm, which are ascribed to transitions from the ${}^2H_{11/2}$ and ${}^4S_{3/2}$ excited states to the ${}^4I_{15/2}$ ground state, respectively. The red emission peak at 654 nm is also observed, which is attributed to the ${}^4F_{9/2}$ to ${}^4I_{15/2}$ transition. The intensity of the red and green emission in β-NaYF₄ microcrystals doped with Er³⁺ and Yb³⁺ ions decreased with increasing concentration of Yb³⁺ from 8 to 32 mol%, which leads to the back-energy transfer (i.e., concentration quenching effect) [30]. As shown in Fig. 4A, the sample Er 32% generates the weakest luminescence emission.

The schematic of energy levels for Yb³⁺ and Er³⁺ ions is given in Fig. 4B. The characteristic emission peaks at 521, 540, and 654 nm are attributed to the ${}^2H_{11/2} \rightarrow {}^4I_{15/2}, {}^4S_{3/2} \rightarrow {}^4I_{15/2}$ and ${}^4F_{9/2} \rightarrow {}^4I_{15/2}$, respectively. The Yb³⁺ ion is an efficient sensitizer for absorbing the excitation energy and then transferring it. As a result, Er³⁺ can populate onto the ${}^4F_{7/2}$ state by absorbing a second 980 nm photon, which can also receive energy from the ${}^2F_{5/2}$ Yb³⁺ state. The ${}^4F_{7/2}$ Er³⁺ can release energy nonradiatively to the ${}^2H_{11/2}$ and ${}^4S_{3/2}$ states, while the ${}^4S_{3/2}$ Er³⁺ may populate onto the ${}^4F_{9/2}$ state via nonradiative multiphonon relaxation and the ${}^4I_{11/2}$ Er³⁺ can populate onto the ${}^4F_{9/2}$ state via transition from ${}^4F_{7/2}$ to ${}^4F_{9/2}$ for the cross relaxation between Er³⁺ ions [31].

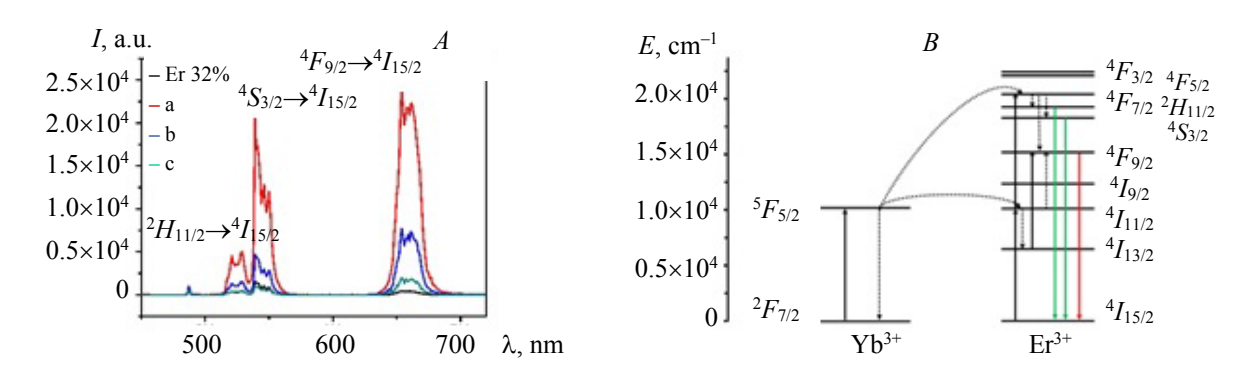


Fig. 4. (A) Up-conversion luminescence of samples Er 32%, a, b, c under excitation of the 980 nm laser; (B) schematic illustration of the energy levels of Yb³⁺ and Er³⁺ ions under 980 nm excitation.

Figure 5 shows the comparative up-conversion luminescence spectra of samples b, d, e, f with the same emission peaks. The other peaks at 490 nm are the diffraction peaks of the 980 nm laser. The peak strength at 654 nm of sample e is 23 times, and for samples b, d it is 9 times. The particle size of the samples having a single crystalline phase has little effect on the luminescence intensity [32]. Sample e has stronger luminescence than samples b and d. This is because the host matrix has the same hexagonal phase, and ions Y³⁺, Lu³⁺, and Yb³⁺ in the host matrix are in the same spatial position. Yb³⁺ as the sensitizer can successively absorb near-infrared (NIR) excitation and transfer the energy to the activators. Sample e can transfer energy to more Yb³⁺ ions around Er³⁺. Yb³⁺ ions or Yb³⁺-Yb³⁺ pairs around Er³⁺ transfer energy to the Er³⁺, inhibiting back energy transfer. Let us verify if Yb³⁺ enhances the luminescence. As seen from Fig. 5B, the peak strength at 654 nm of sample f is 11 times that of sample e. When the concentrations of doped Yb³⁺ and Er³⁺ are high, Yb³⁺ ions in the host matrix can enhance the luminescence more obviously.

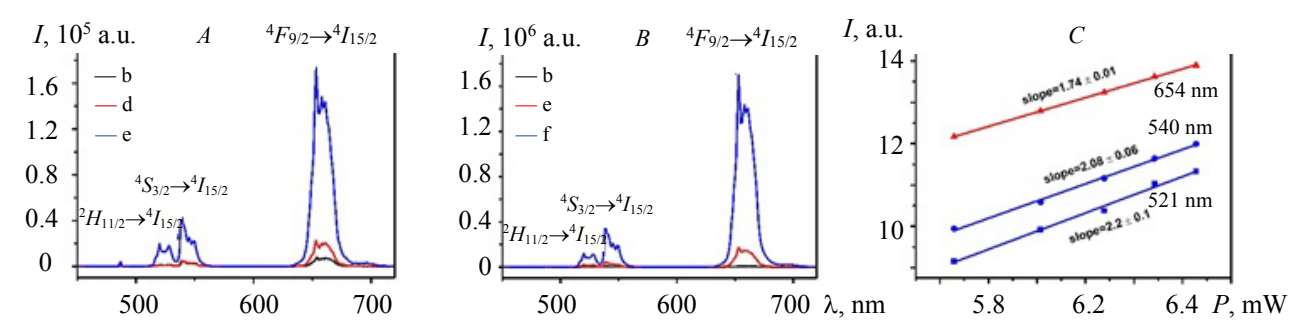


Fig. 5. (A, B) Up-conversion luminescence of samples b, d, e, f and (C) the excitation power-dependence of the up-conversion emission of sample e under excitation of the 980 nm laser.

In order to validate the up-conversion mechanism, the excitation power dependence of up-conversion emissions in sample e is calculated. It is well known that the output up-conversion luminescence intensity is proportional to the infrared excitation power: $I_{\rm UC} \propto I_{\rm IR}^n$, and at low values of $I_{\rm IR}$, n approaches the true value of the number of photons involved in the excitation process [33]. The power dependence of the aforementioned three emission transitions can be obtained from the slope of the fitted line of the plot of $\ln I_{\rm UC}$ versus $\ln(I_{\rm IR})$. As is shown in Fig. 5C, the slopes of the linear fit of $\ln(I_{\rm UC})$ versus $\ln(I_{\rm IR})$ for 521, 540, and 654 nm in sample e are 2.2, 2.08, and 1.74, respectively. The results indicate that only two photon processes are involved to produce the green and red up-conversion emissions. So, using β -NaYbF₄ as the host matrix, one can enhance the luminescence by inhibiting the concentration quenching in the up-conversion luminescence.

The luminescence excitation and decay curves of the samples are presented in Fig. 6. The decay curves are double-exponential. For samples a, b, c, and e, the lifetimes are determined to be 590, 803, 793, and 553 µs, respectively.

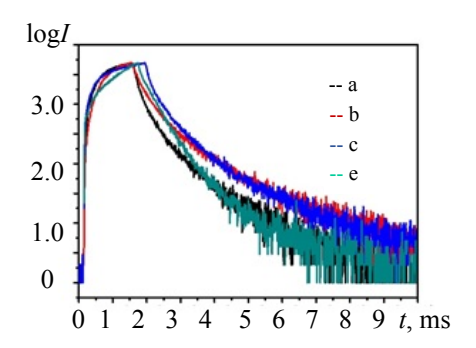


Fig. 6. The luminescence excitation and decay curves of samples a, b, c, e at 540 nm under excitation of the 980 nm laser.

Conclusions. We have developed a facile EDTA-assisted hydrothermal method to synthesize pure β -NaYF₄, β -NaLuF₄, and β -NaYbF₄ microcrystals with high concentrations of Yb³⁺ and Er³⁺ dopants. All the samples have a pure hexagonal phase. The samples with better crystallization have neat morphology. Under excitation of 980 nm radiation, the sample β -NaYbF₄:16 mol% Yb³⁺, 32 mol% Er³⁺ with β -NaYbF₄ as the host matrix has the strongest luminescence. Thus, we have proposed an appropriate method to enhance the up-conversion luminescence of high concentration Yb³⁺, Er³⁺ doped particles.

REFERENCES

- 1. P. Claire, H. Anders, L. Mikael, J. Lumin., 111, 265–283 (2005).
- 2. F. Auzel, Chem. Rev., 104, No. 1, 139–173 (2004).
- 3. Q. B. Wu, S. T. Lin, Z. X. Xie, L. Q. Zhang, Y. N. Qian, Y. D. Wang, H. Y. Zhang, *Appl. Surf. Sci.*, **424**, 164–169 (2017).
- 4. L. Baca, H. Steiner, N. Stelzer, J. Alloys Compd., 774, 418–424 (2019).
- 5. W. Qin, D. Zhang, D. Zhao, L. Wang, K. Zheng, Chem. Commun., 46, 2304–2306 (2010).
- 6. H. S. Qian, H. C. Guo, P. C. L. Ho, R. Mahendran, Y. Zhang, Small, 5, 2285-2290 (2009).
- 7. Y. Zhang, M. M. Li, J. Li, J. Tang, W. J. Cao, Z. N. Wu, Ceram. Int., 44, 22467–22472 (2018)
- 8. N. L. Bel'kova, O. V. Yanush, I. M. Batyaev, L. G. Noskova, M. A. Solov'ev, *J. Appl. Spectrosc.*, 27, 1083 (1977).
- 9. B. Han, B.K. Liu, J. Zhang, H. Z. Shi, J. Mater. Sci., 27, 10742–10746 (2016).
- 10. A. D. Wakeel, A. Zubair, K. Iftikhar, J. Photochem. Photobiol. A: Chem., 356, 502-511 (2018).
- 11. S. M. Maryam, S. Ali, A. Ahmad, S.N. Masoud, J. Clean. Prod., 209, 762–768 (2019).
- 12. D. L. Dexter, J. H. Schulman, J. Chem. Phys., 22, 1063 (1954).
- 13. W. M. Yen, S. Shionoya, H. Yamamoto, *Phosphor Handbook*, 2nd ed., CRC Press, Boca Raton, 106–107 (1999).
- 14. Sushil Kumar Ranjan, Manisha Mondal, Vineet Kumar Rai, Mater. Res. Bull., 106, 66-73 (2018).
- 15. H. Q. Yan, X. Q. Chen, H. W. Song, X. H. Wang, Z. F. Shi, Q. Lin, Mater. Lett., 187, 101–105 (2017).
- 16. R. S. Yadav, R. K. Verma, S. B. Rai, J. Phys. D: Appl. Phys., 46, 275101 (2013).
- 17. J. X. Fu, X. Z. Zhang, Z. C. Chao, Z. B. Li, J. S. Liao, D. J. Hou, H. R. Wen, X. N. Lu, X. R. Xie, *Opt. Laser Technol.*, **88**, 280–286 (2017).
- 18. S. Stevan, T. Nenad, V. Rastko, J. Alloys Compd., 785, 1222–1232 (2019).
- 19. T. Gavrilovic, D. Jovanovic, V. Lojpur, V. Dordevic, M. Dramicanin, J. Solid State Chem., 217, 92–98 (2014).
- 20. Y. Gao, Y. B. Hu, P. Ren, D. C. Zhou, J. B. Qiu, J. Alloys Compd., 667, 297–301 (2016).
- 21. Z. C. Li, D. C. Zhou, Y. Yang, Y. Gao, P. Ren, J. B. Qiu, Opt. Mater., 60, 277–282 (2016).
- 22. F. Zhang, S. W. Wang, X. J. Liu, L. Q. An, X. Y. Yuan, J. Appl. Phys., 105, No. 9, 093542 (2009).
- 23. Y. Wang, X. M. Xie, J. Q. Qi, S. S. Wang, N. Wei, Z. W. Lu, X. T. Chen, T. C. Lu, *J. Lumin.*, 175, 203–206 (2016).
- 24. F. Zhang, S. Chen, H. L. Zhang, J. Li, Y. Yang, G. H. Zhou, X. J. Liu, S. W. Wang, *J. Am. Ceram. Soc.*, **95**, No. 1, 27–29 (2012).
- 25. Q. Y. Huang, W. H. Ye, X. F. Jiao, L.L. Yu, Y. L. Liu, X. T. Liu, J. Alloys Compd., 763, 216–222 (2018).

- 26. P. P. Lei, R. An, X. S. Zhai, S. Yao, L. L. Dong, X. Xu, K. M. Du, M. L. Zhang, J. Feng, H. J. Zhang, J. Mater. Chem. C, 5, 9659–9665 (2017).
- 27. S. Ye, P. Xiao, H. Z. Liao, S. Li, D. P. Wang, Mater. Res. Bull., 103, 279–284 (2018).
- 28. M. Ding, D. Chen, D. Ma, J. Dai, Y. Li, Z. Jia, J. Mater. Chem. C, 4, 2432–2437 (2016).
- 29. Z. D. Ivana, T. M. Lidija, E. R. Maria, Y. Kazuhiro, O. Satoshi, T. Sayaka, K. Tomita, M. C. Antonio, A. M. Bojan, B. M. Olivera, *Adv. Powder Technol.*, **28**, 73–82 (2017).
- 30. S. Hinojosa, M. A. Meneses-Nava, O. Barbosa-Garcia, L. A. Diaz-Torres, M. A. Santoyo, J. F. Mosino, *J. Lumin.*, **102-103**, 694–698 (2003).
- 31. K. Wang, J. Jiang, S. Wan, J. Zhai, Electrochim. Acta, 155, 357–363 (2015).
- 32. Y. Wang, S. L. Gai, N. Niu, F. He, P. P. Yang, Phys. Chem. Chem. Phys., 15, 16795–16805 (2013).
- 33. M. T. Berry, P. S. May, J. Phys. Chem. A, 119, 9805–9811 (2015).